Behaviour of Z-Shape Steel Plate Shear Connectors Used in Concrete Sandwich Wall Panels

N. Goudarzi, PhD Candidate in Structural Engineering, University of Alberta, Alberta, Canada
Y. Korany, Former Associate Professor of Structural Engineering, University of Alberta, Alberta, Canada
S. Adeeb, Associate Professor of Structural Engineering, University of Alberta, Alberta, Canada
R. Cheng, C.W. Carry Professor of Steel Structures, University of Alberta, Alberta, Canada

Abstract: Concrete Sandwich Wall Panels (CSWP) consist of two concrete layers with insulation in between. They provide thermal and acoustic insulation and protect the building from moisture ingress. These prefabricated CSWP are widely used in North America to enclose buildings and are subject to high out-of-plane wind and seismic loads. Under out-of-plane loading, CSWP may behave as non-composite, semi-composite or fully-composite panels. The degree of this out-of-plane flexural composite action depends significantly on the shear behaviour of the mechanical connectors between the concrete layers. A CSWP with higher degree of composite action has substantially higher out-of-plane flexural resistance. Hence, the shear response of interlayer mechanical connectors should be optimized to maximize the out-of-plane composite action of CSWP.

Due to their high efficiency in mobilizing out-of-plane flexural composite action, Z-Shape Steel Plate Connectors (Z-SPC) have recently been used as interlayer mechanical connectors in CSWP. This paper reports the findings of an experimental program to characterize the shear behaviour of Z-SPC. The experimental strength and stiffness of seven push-out shear tests on Z-SPC were compared against two analytical models. The tested Z-SPC had different widths and thicknesses. Both the physical and analytical models were used to investigate the effect of the width and thickness of Z-SPC on their shear strength and stiffness. The effect of cracking of concrete at the connector-concrete interface was also investigated. It was found that cracking and debonding at the connector-concrete interface reduces the shear strength and stiffness of Z-SPC, and this effect increases with thickness of the connectors. The findings of this investigation will be used to optimize the design of Z-SPC and accurately predict the out-of-plane flexural behaviour of CSWP constructed using Z-SPC.

1 INTRODUCTION

Out-of-plane behaviour of Concrete Sandwich Wall Panels (CSWP) significantly depends on the shear strength and stiffness of their interlayer mechanical connectors. The connectors with sufficient shear strength and stiffness to mobilize semi-composite or fully-composite action in CSWP are called shear connectors. Some common types of shear connectors include truss connectors, Fibre Reinforced Polymer (FRP) grid connectors, expanded metal shear connectors and connecting concrete regions between the concrete layers. Truss connectors can mobilize high degree of composite action if oriented in the longitudinal direction of the panel (Salmon et al. 1997, Einea 1992, Peifer and Hanson 1964). Under out-of-plane loading, high tensile and compressive forces develop in the web members of truss connectors near the ends of CSWP. Steel truss connectors have more ductile behaviour than FRP truss connectors (Salmon et al. 1997). Web members of truss connectors are prone to buckling near the ends of CSWP. Shear behaviour of expanded metal connectors and GFRP grid connectors have been studied previously (Soriano and Rizkalla 2013, Natio et al. 2012, Mouser 2003). Grid connectors fail under buckling of compressive chords and rupture of tensile chords, however they produce semi-composite action in CSWP (Soriano and Rizkalla 2013). Tri-linear force-displacement behaviour has been proposed for different types of connectors including steel truss and GFRP grid connectors by Naito et al. (2012). Concrete regions have also been investigated and found to be very efficient in mobilizing composite

action (Pessiki and Mlynarczyk 2003, Peifer and Hanson 1964), however they significantly reduce the thermal efficiency of the panel due to bridging.

A new mechanical connector system for CSWP has recently been developed using Z-shape Steel Plate Connectors (Z-SPC) partially embedded in concrete, the structural behaviour of which has not yet been studied. Due to high in-plane shear and flexural strength and stiffness of Z-SPC, this type of connector is structurally more efficient in providing interlayer shear strength and stiffness in CSWP. In a preliminary study (Goudarzi et al. 2014) on CSWP under out-of-plane 4-point loading, this connector system proved to efficiently mobilize full-composite action. However, to optimize the dimensions and number of Z-SPC to be used in CSWP, the shear behaviour of these connectors should be known. Therefore, in this study the shear behaviour of Z-SPC with different widths and thicknesses is experimentally investigated. These experimental results are compared with two theoretical models that can be used to predict the shear response of these connectors.

2 EXPERIMENTAL INVESTIGATION

Seven push-out shear tests on three groups of connectors were conducted on 76.2 mm and 101.8 mm wide Z-SPC connectors made of gauge #16 and gauge #10 steel sheets. The groups of connectors are annotated hereafter as SHα-β, where α is the width of the Z-SPC in inches and β is the gauge number of the steel sheet. The geometric and material properties of the connector groups are given in Table 1. As shown in this table, the results of three replicas of SH3-16 and two replicas of each connector groups SH4-16 and SH4-10 are reported in this paper. One specimen in SH4-16 and one in SH4-10 connector groups had different specifications due to construction errors, therefore their results are not reported here. Individual specimens are referred to as SHα-β-γ, where γ is the number of specimen. Figure 1 shows that push-out shear specimens consisted of three concrete layers encasing two layers of insulation. The side concrete layers and the middle concrete layer were 76.2 mm and 152 mm thick, respectively. The middle concrete layer was connected to each of the side concrete layers by one Z-SPC. The concrete layers were reinforced by three Grade 400 10M rebars and the connectors were tied to the rebars. The insulation consisted of one 51.6 mm layer of Polystyrene foam panel and one 25.4 mm layer of grooved Styrofoam bead board.

Table 1: Geometric and material properties of tested connector groups.

Connector Group	Number of Replicas	Gauge Number of steel sheet	Thickness (t) mm	Width (W) mm	f_y MPa	f_u MPa
SH3-16	3	16	1.47	76.2	350	470
SH4-16	2	16	1.47	101.6	195	320
SH4-10	2	10	3.22	101.6	308	430

No standard test method for interlayer mechanical connectors of CSWP was found in the existing design codes. To derive shear behaviour of Z-SPC in this study, the specimens were positioned on a pedestal and the middle concrete layer was pushed down by a hydraulic jack. Since these connectors have low torsional stiffness, they were prone to twisting as shown in Figure 2. Therefore, a wooden containment box was used to restrain the middle layer from twisting during the test, as seen in Figure 3.

Two steel rods were connected to the sides of the middle concrete layer using drop-in anchors, and two cable transducers were tied to these rods to record the vertical displacement of the middle concrete layer. A 25.4 mm thick steel plate was used to transfer the jack load to the middle layer. This plate was levelled on the middle concrete layer before the start of the test using plaster of Paris.

28-day compressive strength of the concrete of these shear specimens was measured using 50.0 mm by 101.6 mm concrete cylinders. The 28-day compressive strength, secant modulus of elasticity and Poisson ratio of the concrete were 41.77 MPa with 4% coefficient of variation, 24.47 GPa and 0.171, respectively. Also the results of eleven split tests on the same size concrete cylinders showed that the tensile strength of concrete was 3.83 MPa with 12.6% coefficient of variation. Three tensile steel coupons cut from each

connector group, i.e. total of 9 coupons, and three compressive foam specimens were tested according to ASTM A370-13 and ASTM C165-07, respectively. The stress – strain behaviour of steel coupons and insulation material are shown in Figure 4. and Figure 5, respectively.

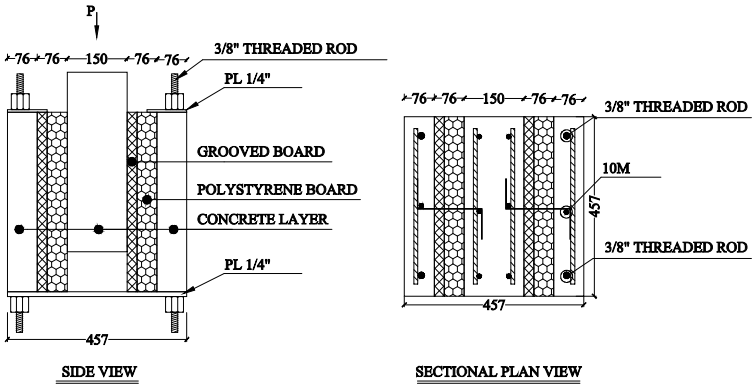

Figure 1: Schematic of push-out shear tests. Units are in (mm)

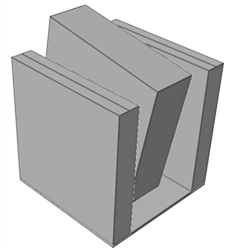

Figure 2: Twisting of middle concrete layer.

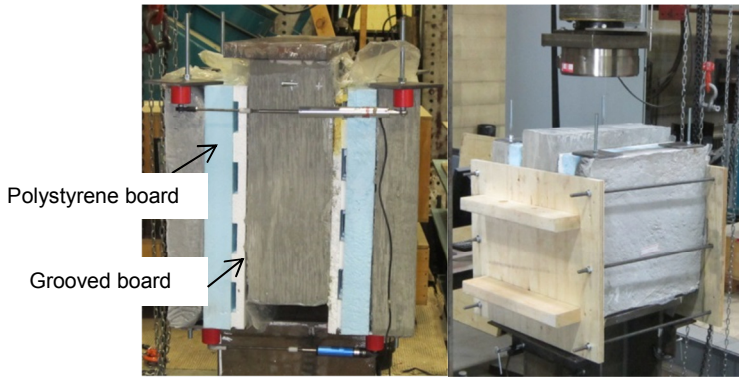

Figure 3: Test setup for push-out tests.

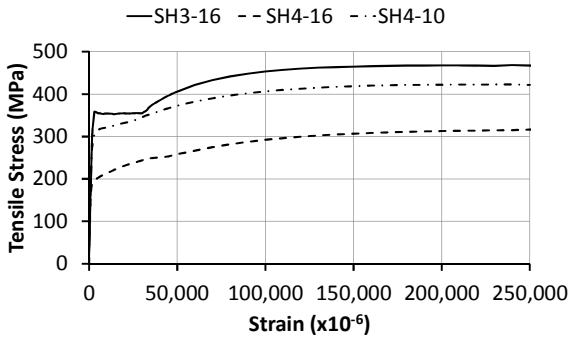

Figure 4: Stress-strain behaviour of steel sheet.

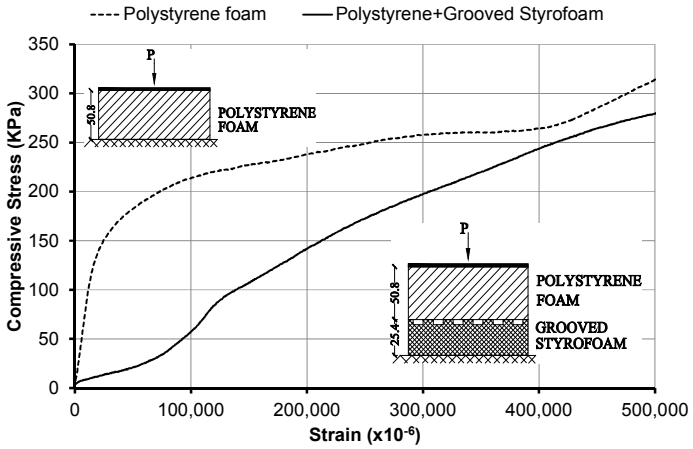

Figure 5: Compressive behaviour of polystyrene and grooved board.

3 TEST RESULTS AND DISCUSSIONS

Test results are summarized in Table 2 and shown in Figure 6. Figure 6 shows the shear force (V) carried by one connector versus the vertical displacement (Δ_v) of the middle concrete layer for the three connector groups. Table 2 summarizes the experimental results for these connector groups. From Figure 6.a., the shear forces of the Z-SPC in SH3-16 specimens reach the average peak shear strength ($V_{r,exp}$) of 13.58 kN at $\Delta_v = 2.2$ mm, after which they slowly drop to 8.0 kN except for SH3-16-3, where the shear force remain constant at 12.0 kN. As shown in Figure 6.b. the connectors in SH4-16 specimens reach their maximum shear strength of 13.5 kN at Δ_v =1.9 mm after which the shear resistance slowly decreases to 10 kN and remain constant. As shown in Figure 6.c. both connectors SH4-10-1 and SH4-10-2 have the same behaviour up to Δ_v =3.0 mm, where the shear force in both specimens reaches to about 35 kN. Subsequently the shear force in SH4-10-1 continues its ascent with a small slope and reaches the maximum shear resistance of 37 kN, and suddenly drops to 20 kN at Δ_v =8.3 mm, whereas the shear force in SH4-10-2 slowly decreases to 22 kN after Δ_v =3.0 mm with multiple drops on the way.

The shear behaviour of SH4-10 shows multiple sudden drops after the peak shear force, which is not observed in the shear behaviour of SH3-6 and SH4-16. This ragged pattern may be attributed to concrete cracking at connector-concrete interface, which is more pronounced for SH4-10 connectors. The connectors used in SH4-10 have a higher thickness than SH3-16 and SH4-16 connectors, thus transfer higher forces and moments to the concrete resulting in higher stress concentrations in concrete. This, in turn, results in intense concrete cracking at the interface. However, when the width of connector is increased, its strength and stiffness is improved, while the connector-concrete contact area expands proportional to the width. Thus, the higher forces and moments of the connector are transferred to a larger concrete area, reducing concrete cracking.

Table 2 shows that experimental shear stiffness of the tested connectors (K_{exp}), derived from linear portion of the $V_{r,exp} - \Delta_v$ graphs, increases with their width and thickness. From connectors in SH3-16 to those in SH4-16, the width and K_{exp} increase by almost 33%. And from connectors in SH4-16 to those in SH4-10, the thickness and K_{exp} increase by 100% and 75%, respectively. This shows that increase in thickness of connectors rather than width has lower impact on K_{exp}, which may be ascribed to intensified stress concentrations and consequent concrete cracking as the thickness is increased.

Figure 7 illustrates the failure mode of the connectors in the tested connector groups after the test and shows that all connectors underwent significant buckling and developed a tension field. This post-failure tension field can explain the ability of the specimens to carry significant shear forces after the peak. As shown in figures 6 and 8 in all connector groups the shear force decreased and remained steady, which can indicate tension-field action as shown in Figure 7.

Table 2: Summary of push-out test results.

Z-SPC Designation		SH3-16	SH4-16	SH4-10
Experimental yield stress of steel sheet	f_y (MPa)	350	195	308
Yield shear resistance (MPa)	$\tau_y = f_y/\sqrt{3} =$	202	113	178
Experimental Ultimate shear resistance	$V_{r,exp}$ (kN)	13.58	13.50	36.18
Experimental shear stiffness (V/Δ_v) derived from linear part of $V - \Delta_v$ graph	K_{exp} (kN/mm)	11.05	14.80	25.97

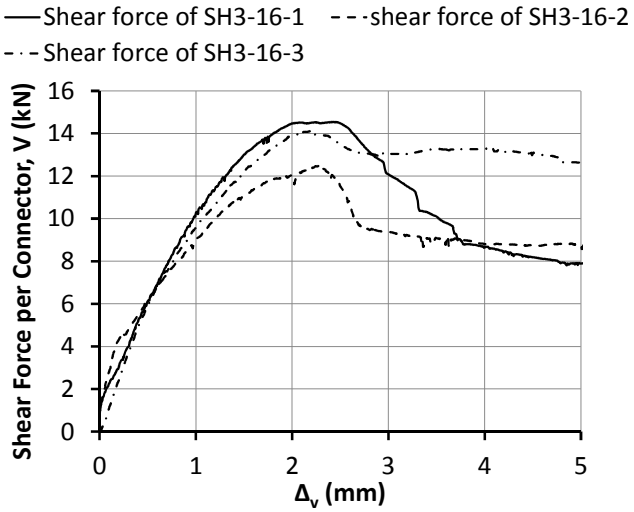

a. SH3-16

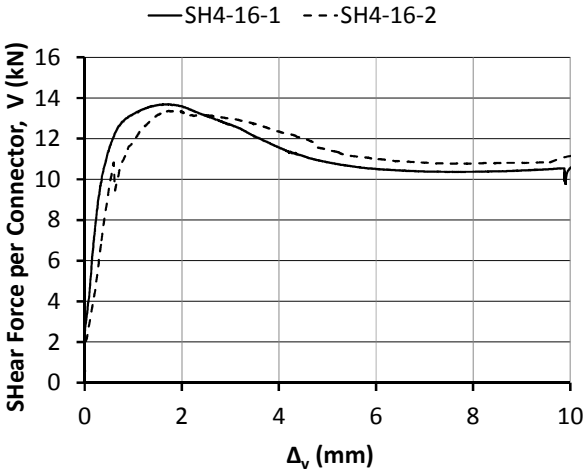

b. SH4-16

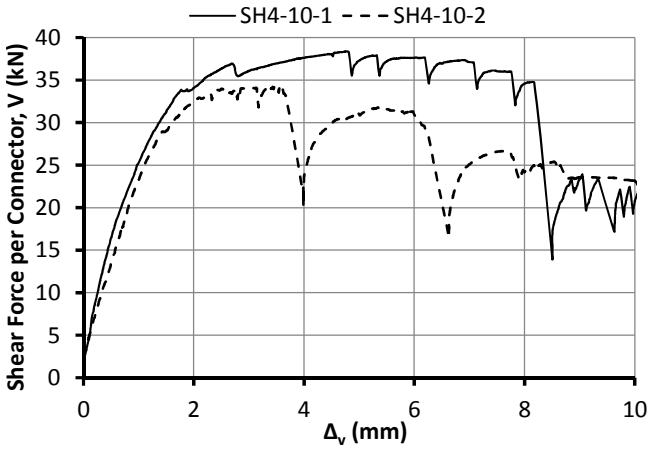

c. SH4-10

Figure 6: Connector shear force vs. Δ_v for a. SH3-16, b. SH4-16 and c. SH4-10 connector groups.

a. SH3-16

b. SH4-16

c. SH4-10

Figure 7: Buckling of Z-SPC.

4 ANALYTICAL INVESTIGATION

Shear behaviour test results were compared to estimates from two theoretical models: simplified plate model and idealized beam model. In the first model the connector is simplified as a steel plate assumed to be embedded in two fixed concrete layers while one concrete layer is pushed down as shown in Figure 8.a. In this model, under loading the top right and bottom left corners are under flexural compressive stresses. As the loading increases, buckling starts from these compression corners and spreads throughout the connector, forming a tension field mechanism. If the steel sheet is very thin buckling of these corners governs the maximum shear resistance of Z-SPC. Since the shear behaviour of this simplified plate model bears resemblance to shear tabs in steel structures, the analytical method proposed by Muir and Thornton (2004) for the buckling resistance of shear tab connections is adopted to analyze the tested Z-SPC. In this method, a slenderness parameter λ is defined by Eq. 1.

$$[1]\ \lambda = \frac{W\sqrt{f_y}}{10t\sqrt{475+280(W/L)^2}}$$

Where t, W and L are defined in Figure 8. and f_y is the yield stress of the steel plate. In this method if $\lambda < 0.7$, buckling is not the governing mode of failure (Muir and Thornton, 2004). If the thickness of the simplified plate model is sufficiently high, yielding of the plate governs the shear behaviour of the connector. Tresca yield criterion is adopted to calculate the lower and upper bound shear strengths of the simplified plate, $V_{r,lower}$ and $V_{r,upper}$, based on fully plastic section of a rectangular plate under moment about one axis and shear force. Lower and upper bound shear strengths are calculated using Eq. 2 and Eq. 3, respectively, as presented by Drucker (1956).

$$[2]\ \frac{M}{M_0} + \frac{3}{4}\left(\frac{V_r}{V_0}\right)^2 = 1$$

$$[3]\ \frac{M}{M_0} + \left(\frac{V_r}{V_0}\right)^4 = 1$$

Where M is the exerted moment on the beam section, i.e. $M = V_r\, L/2$, M_0 is the plastic moment, i.e. $M_0 = 0.25 f_y t W^2$, and V_0 is the plastic shear resistance, i.e. $V_0 = 0.5 f_y t W$.

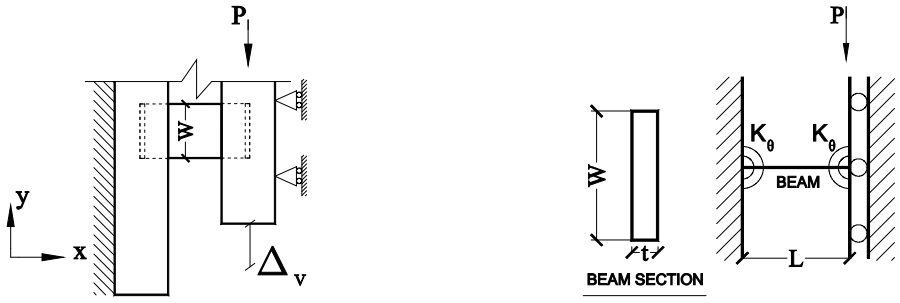

a. Simplified plate model b. Idealized beam model

Figure 8: Theoretical models for the analysis of the tested shear specimens.

In the second model the connector is idealized as a beam of length L, that is equal to the thickness of insulation, width t and depth W connected to end rigid supports by rotational springs with the stiffness K_θ, as shown in Figure 8.b. These rotational springs represent connector-concrete interaction, i.e. cracking of concrete and debonding at connector-concrete interface. Von Mises criteria (Eq. 4) is used to establish the yield criteria for the beam.

$$[4]\ \sigma_{VM} = \sqrt{1/2 \times \left[(\sigma_{xx}-\sigma_{yy})^2 + (\sigma_{xx}-\sigma_{zz})^2 + (\sigma_{yy}-\sigma_{zz})^2\right] + 3(\tau_{xy}^2 + \tau_{xz}^2 + \tau_{yz}^2)}$$

Where σ_{xx}, σ_{yy} and σ_{zz} are the normal stresses, τ_{xy}, τ_{xz} and τ_{yz} are the shear stresses in a three dimensional state of stress, and f_y is the tensile yield stress. The shear connectors in this study are assumed to be under a two dimensional state of stress, i.e. the applied stresses on the connectors are only τ_{xy} and σ_{xx}. Here, the normal and shear stresses are assumed to have linear and uniform distributions, respectively, over the depth of the idealized beam. Thus, $\sigma_{xx} = 3V_yL/(tw^2)$ and $\tau_{xy} = V_y/(tW)$, where V_y is the yield shear strength of the connector estimated by the idealized beam model using Von Mises criteria. It should be noted that these assumptions for shear and normal stresses are taken only to simplify the problem, and does not reflect the exact stress distributions in the tested shear connectors. Exact stress distribution in the connectors could be determined by Finite Element Analysis (FEA). Also, the length of the idealized beam is taken as the thickness of the insulation. However, debonding at the concrete-concrete interface increases the length of the connector under shear force, which changes the estimated V_y. This beam model is developed to understand how experimental shear behaviour of Z-SPC differs from estimated behaviour from an ideal beam. This understanding and future FEA results can lead to a modified beam model to be used for structural design of Z-SPC under shear forces.

5 ANALYTICAL RESULTS AND DISCUSSIONS

Table 3 summarizes the comparison between the theoretical predictions and test results, and it gives the percentage difference between experimental results and the estimated ones from the two theoretical models. Table 3 shows that $\lambda < 0.7$ for all of the connectors in this study, thus buckling does not govern their failure. It should be noted that out-of-plane deformation in SH3-16 and SH4-16 might have started at their peak shear forces, but it did not cause premature buckling failure as predicted by Eq. 1. Table 3 also compares theoretical lower and upper bound shear strengths, $V_{r,lower}$ and $V_{r,upper}$, with the experimental shear strength. The maximum difference of estimations by $V_{r,lower}$ and $V_{r,upper}$ are 18.6% and 14.5%, respectively. The upper and lower bound theories show highest accuracy in predicting shear strength of SH3-16 and lowest accuracy in that of SH4-16. Table 3 also shows that $V_{r,exp} > V_{r,upper}$ for SH4-16 and $V_{r,exp} < V_{r,lower}$ for SH4-10. This implies that SH4-16 connectors had higher plastic capacity than estimated by upper bound theory (Eq. 3), which can be attributed to tension-field action of the plate. Also SH4-10 connectors had lower plastic capacity than estimated by lower bound theory (Eq. 2), which may relate to intense cracking of concrete at connector-concrete interface.

Table 3 shows that shear strength ratio, $V_{r,exp}/V_y$, for all connector groups, where V_y is the yield shear strength of the idealized beam using Von Mises yield criteria. Shear strength ratio shows the extent by which the shear strength (peak shear force) of the connector exceeded the yield shear strength of the connector estimated by the idealized beam model using Von Mises yield criteria. If this ratio is higher than one, it means the connector has some "post-yield" shear capacity. Table 3 shows that the shear strength ratios for SH3-16 and SH4-16 connectors are 1.19 and 1.33, respectively. This demonstrates the post-yield shear capacity of these connectors, which may be attributed to plastic deformation and tension-field action in the connector material. It also shows that SH4-16 has higher post-yield shear capacity than SH3-16, which may imply that a wider connector exhibits higher post-yield shear capacity. This may be explained by higher shear stresses in a wider connector that leads to higher shear yielding and tension-field action, resulting in higher post-yield shear capacity.

Table 3 shows that $V_{r,exp}/V_y = 1.02$ for SH4-10 connectors, meaning almost no post-yield capacity. This might be due to higher thickness of SH4-10 connectors and the associated higher stress concentration on the concrete around the connector-concrete interface. As mentioned earlier, higher thickness of connector improves shear strength and stiffness of the connector without sufficiently expanding the connector-concrete contact area, which generates high stress concentrations in the concrete, leading to intense cracking and lowered shear resistance. This might also explain the lack of post-yield shear capacity for this connector group. The described intensive cracking of concrete prevents plastic deformations of the connector, therefore the global failure occurs just after yield stress is reached in the material.

Table 3: Comparison of experimental and theoretical results.

Z-SPC Designation		SH3-16	SH4-16	SH4-10
Slenderness parameter (Eq. 1)	λ	0.126	0.098	0.056
Lower bound shear resistance (Eq. 2)	$V_{r,lower}$ (kN)	13.20	10.99	38.19
	Difference (%)	2.79	18.59	5.56
Upper bound shear resistance (Eq. 3)	$V_{r,upper}$ (kN)	14.35	11.54	40.12
	Difference (%)	5.65	14.49	10.89
Yield shear strength using Von Mises criteria (Eq. 4)	V_y (kN)	11.43	10.21	35.48
Shear strength ratio	$V_{r,exp}/V_y$	1.19	1.33	1.02
Stiffness of idealized beam	K_{beam} (kN/mm)	77.51	124.04	263.02
Stiffness ratio	K_{exp}/K_{beam}	0.14	0.12	0.10

To assess the effect of connector–concrete interaction on the shear stiffness of the tested Z-SPC, the idealized beam model shown in Figure 8.b. was used. The stiffness of this idealized beam with fixed ends K_{beam} is $[L^3/(12EI) + L/(GA)]^{-1}$, where I is the moment of inertia of the cross section of this idealized beam in Figure 8.b. Micro-cracking of the concrete and debonding at the connector-concrete interface reduces the overall shear stiffness of the connector, which is included in the stiffness of end rotational springs in the idealized beam. Table 3 shows that the stiffness ratio K_{exp}/K_{beam} for the three connector groups decreases from 0.14 for SH3-16 with lowest cross sectional area to 0.10 for SH4-10 with highest cross sectional area. This suggests that due to connector–concrete interaction, including debonding and cracking, the experimental shear stiffness of Z-SPC is significantly lower than that estimated by the idealized beam model.

6 CONCLUSION

Shear behaviour of interlayer mechanical connectors significantly affects out-of-plane behaviour of Concrete Sandwich Wall Panels (CSWP). In this study, the shear behaviour of Z-shape Steel Plate Connectors, recently utilized in CSWP, was assessed by seven push-out shear tests on three types of Z-SPC. These experimental results were compared with two theoretical models to evaluate the effect of width and thickness of these shear connectors on their shear strength and stiffness. The experimental results show that the connector-concrete interaction significantly affects the shear strength and stiffness of Z-SPC connectors. Increasing the width was found to be more effective in improving the shear resistance of the connectors. Concrete cracking and debonding at connector-concrete interface significantly reduces the shear stiffness of the connectors, and this effect increases with increased cross sectional dimensions. Also, the experimental and analytical results suggest that Z-SPC with higher thickness/width ratio can generate high stress concentration and micro-cracking in the concrete around the embedded portion of the connector, which lowers the shear strength and stiffness of the connector. If these stress concentrations are prevented by choosing the right thickness/width ratio Z-SPC can show up to about 30% post-yield shear capacity. The upper bound theory using Tresca yield criteria estimates the shear resistance of the tested Z-SPC connectors with about 19% difference. A simplified model using an idealized beam was introduced and shown to be effective in interpreting the experimental results. This model can be further developed to predict the shear resistance of Z-SPC connectors with higher accuracy.

7 ACKNOWLEDGEMENTS

The first author was funded by Natural Sciences and Engineering Research Council of Canada (NSERC) through an industrial sponsorship from Read Jones Christoffersen (RJC) Consulting Engineers. The experimental studies reported in this paper were conducted in I.F. Morrison's Structures Laboratory at University of Alberta.

8 REFERENCES

ASTM (2013). ASTM A370-13: Standard Test Methods and Definitions for Mechanical Testing of Steel Products. *Annual Book of ASTM Standards*, ASTM International, West Conshohocken, Pennsylvania, USA.

ASTM (2012). ASTM C165-07: Standard Test Methods for Measuring Compressive Properties of Thermal Insulation. *Annual Book of Standards*, ASTM International, West Conshohocken, Pennsylvania, USA.

Drucker, D. C. (1956). The effect of shear on the plastic bending of beams. *Journal of applied mechanics*, Volume 23, p. 509-514.

Einea, A.A., (1992). *Structural and Thermal Efficiency of Precast Concrete Sandwich Panel Systems*, PhD Thesis, University of Nebraska, Lincoln, Nebraska, USA.

Goudarzi, N., Hatzinikolas, M. and Korany, Y. 2014. Out-of-Plane Behaviour of Precast Concrete Sandwich Wall Panel Systems. *4th Annual International Conference on Civil Engineering*, The Athens Institute for Education and Research, Athens, Greece.

Maximos, H. N., Pong, W. A., Tadros, M. K., Martin, L. D. (2007). *Behavior and Design of Composite Precast Prestressed Concrete Sandwich Panels with NU-Tie*, University of Nebraska, Lincoln, Nebraska, USA.

Mouser, L.A.D. (2003). *Partially Composite concrete Sandwich Panels,* M.S. Thesis, University of Alberta, Edmonton, Alberta, Canada.

Muir, L. S. and Thornton, W. A. (2004). A Direct Method for Obtaining the Plate Buckling Coefficient for Double-Coped Beams. *Engineering Journal*, AISC, 3rd Quarter, pp. 133-134.

Naito, C., Hoemann, J., Beacraft, M., Bewick, B., (2012). Performance and Characterization of Shear Ties for Use in Insulated Precast Concrete Sandwich Wall Panels. *Journal of Structural Engineering*, ASCE, Vol. 138, pp. 52-61.

Peifer, D. W., Hansen, J. A. (1964). Precast Concrete Wall Panels: Flexural Stiffness of Sandwich Panels. *Special Publication, SP-11*, American Concrete Institute (ACI), Farmington Hill, Michigan, USA, pp. 67-86.

Pessiki, S., Mlynarczyk, A., (2003). Experimental Evaluation of Composite Behavior of Precast Concrete Sandwich Wall Panels. *PCI Journal*, March-April, pp. 54-71.

Salmon, D. C., Al-Einea, A., Tadros, M. K., Culp, T. D., (1997) Full Scale Testing of Precast Concrete Sandwich Panels. *ACI Structural Journal*, Vol. 94, No. 4, pp. 354-362.

Soriano, J., Rizkalla, S., (2013). Use of FRP Grid for the Composite Action of Concrete Sandwich Panels. *11th International Symposium on Fiber Reinforced Polymer for Reinforced Concrete Structures (FRPRCS11)*, Guimaraes, Portugal.